DOI: 10.1002/cphc.200900340

Femtosecond Measurements of Vibrational Circular Dichroism and Optical Rotatory Dispersion Spectra

Hanju Rhee,[a, c] Seong-Soo Kim,[a] Seung-Joon Jeon,[b, c] and Minhaeng Cho*[a, c]

Vibrational optical activity (VOA) is a chiroptical property originating from nuclear vibrations of chiral molecules.[1–4] Consequently it is highly sensitive to molecular conformations and provides valuable information on absolute configuration of chiral molecules such as proteins, nucleic acids, and asymmetrically synthesized drugs in condensed phases.[5–7] Recently, we developed a novel vibrational optical activity free-induction-decay (VOA FID) measurement technique,[8–10] as an alternative to overcome the weak signal and non-zero background problems of traditional vibrational circular dichroism (VCD) measurement method. A combined cross-polarization and heterodyned detection scheme employed in such technique significantly boosts the chiral sensitivity. In addition, its potential capability of femtosecond time-resolution makes it possible to monitor the chirality change of molecular systems in ultrafast motion.

A success of the VOA FID measurement strongly depends on optical perfectness of the cross-polarization configuration. Real polarizers, however, have finite (non-zero) extinction ratio (ER) and the achiral FID thus leaked through such a cross geometry could substantially contaminate the pure chiral signal. For typical chiral samples, differential absorbance ΔA (VCD) is about 10^{-4} times smaller than the absorbance itself. In this case, high quality polarizers with ER smaller than $\sim 10^{-8}$ are needed to discriminate such a weak VOA signal from the large achiral background. Although the previous experimental setup enabled us to examine the C–H stretching VCD-active modes (2830 ~3000 cm^{-1}) of organic chiral molecules,[9,10] it still poses a serious technical problem: the exceptional ER ($\sim 10^{-9}$) of the dichroic absorptive calcite polarizers used is achieved at only restricted IR frequency ranges.[11] The spectral limitation imposed by the effective working frequency range of the calcite polarizer thus confines our scope to the C–H stretching vibrations only and therefore precludes versatile applications to the studies of other vibrations. Indeed, the C=O stretching vibration (amide I mode, 1600 ~ 1700 cm^{-1}) of proteins and polypeptides has been more extensively studied to interrogate their secondary structures.[5,12–14]

In this regard, the reflective Brewster's angle germanium polarizer (BAGP) that was designed and characterized previously[15] can be of critical use in a wide range of applications of the cross-polarization VOA FID measurement technique. BAGP consists of four germanium windows arranged in a chevron-geometry (Figure 1 a), where the incident beam is reflected four times at germanium windows at the Brewster's angle (θ_B).

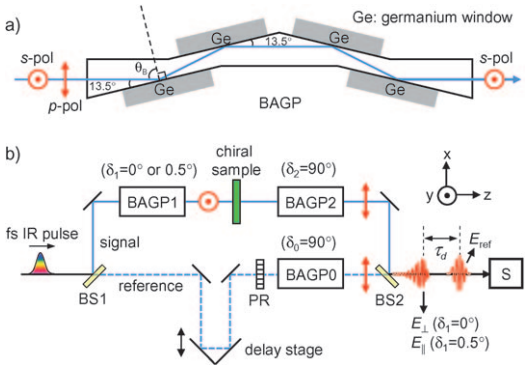

Figure 1. a) Chevron-geometry Brewster's angle germanium polarizer (BAGP). Photographic image of BAGP is shown in the Supporting Information. b) Heterodyned spectral interferometric VOA FID measurement setup. BAGP0-2, polarizers shown in (a); δ_{0-2}, the angle between the transmission axis of BAGP0-2 and *y*-axis; BS1-2, beam-splitters; PR, polarization rotator; S, spectrometer. The reference field (E_{ref}) precedes the FID signal field ($E_{\perp,||}$) by a time delay τ_d.

As a yardstick of high performance polarizer, the large major transmittance and the small ER are required. Since germanium has a high index of refraction ($n \cong 4$), the transmittance of *s*-pol (major transmission field) is fairly large (~0.4) even after four reflections. In addition, due to nearly constant refractive index of germanium from the near to the far IR, the Brewster's angle giving the reflectance minimum of *p*-pol (minor transmission field) does not significantly change over almost entire IR frequency range. According to the previous calculation, with a 35-mrad half-angle beam divergence and $\theta_B = 76.5°$, it was shown that the ER is smaller than 10^{-9} from $\lambda = 1$ to beyond 500 μm.[15]

From the previous studies, we found that the complex optical activity susceptibility, $\Delta\chi(\omega)$, whose imaginary and real parts are related to the CD and optical rotatory dispersion (ORD), respectively, is proportional to the ratio of perpendicular $E_\perp$ (VOA FID) to parallel $E_{||}$ (achiral FID) with respect to the incident electric field polarization.[8–10] For a complete characterization of $\Delta\chi(\omega)$, therefore, both FID fields should be inde-

[a] Dr. H. Rhee, S.-S. Kim, Prof. M. Cho
Department of Chemistry and Center for Multidimensional Spectroscopy
Korea University, Seoul 136-701 (Korea)
Fax: (+82)-2-3290-3121
E-mail: mcho@korea.ac.kr

[b] Prof. S.-J. Jeon
Department of Chemistry
Korea University, Seoul 136-701 (Korea)

[c] Dr. H. Rhee, Prof. S.-J. Jeon, Prof. M. Cho
Multidimensional Spectroscopy Laboratory
Korea Basic Science Institute, Seoul 136-713 (Korea)

Supporting information for this article is available on the WWW under http://dx.doi.org/10.1002/cphc.200900340

pendently measured through the heterodyne-detection scheme (Figure 1b), where the spectral beat signal produced by the interference between each FID field and a preceding reference field by a fixed time delay (τ_d) is recorded as the respective spectral interferogram ($S_{\perp,||}$). An interesting advantage of using the relationship, $\Delta\chi(\omega) \propto E_\perp/E_{||}$, is that neither reference field characterization nor precise τ_d determination is needed because the phase contributions from τ_d and the reference field cancel out when the ratio $E_\perp/E_{||}$ is calculated.[9,10] Instead, there is a prerequisite for such cancellation: the optical path difference between the reference (blue dashed) and signal (blue solid) paths that determines the τ_d value should not be altered during the two measurements ($\delta_1 = 0°$, $0.5°$). Other typical birefringence-type prism-polarizer usually makes the input beam displace and deviate from the propagating optic axis. Consequently, its rotation may cause a significant optical path change in terms of the optical wavelength. In the present case of the chevron-geometry polarizer, however, the beam path is ideally rotationally-invariant and alignment-insensitive due to its own geometrical advantage. These two outstanding features make the BAGP applicable to the wide-band VOA FID measurement experiment.

To verify that the VOA FID measurement employing the home-made BAGP's above is experimentally feasible, we carried out an experiment on (1S)-β-pinene in its C–C stretch vibration region (1100 ~1400 cm^{-1}). Note that this frequency range is definitely outside the working frequency range of the dichroic calcite plate polarizer previously used. The experimental setup shown in Figure 1b is similar to the previous one except that three BAGP's are used. The heterodyned spectral interferograms (red solid) of neat (1S)-β-pinene solution in a calcium fluoride sample cell are plotted in Figure 2a. The difference between $S_\perp$ (upper, red) and $S_{||}$ (lower, red) is clearly notable and their spectral features contain information on the chiral and achiral FID signals, respectively.

Nevertheless, it should be mentioned that the perpendicular-detected spectral interferogram $S_\perp$ (upper, red) of the chiral sample includes the contributions from the polarizers and the sample cell itself. The present crossed polarizer pair (BAGP1 and BAGP2), even though its extinction ratio is sufficiently small, is not perfect yet so that there exists a small leaked beam contributing to the measured interferogram even in the absence of the chiral sample. In addition, the calcium fluoride cell is not perfectly amorphous and has small local anisotropy, which is large enough to alter the beam polarization state and consequently such a leaked light contaminates the signal. Fortunately, however, by optimally controlling the cell rotation, the two adverse effects can be compensated with each other to minimize the leakage level. To see this background field effect, the perpendicular detection was performed for the cell itself and the resultant spectral interferograms (blue dashed lines) are depicted together in Figure 2a. Despite the maximal suppression of background contribution, its magnitude appears to be comparable to that of the chiral signal for the chiral solution sample. However, since the combined polarizer-cell contribution appears just as a slowly-varying baseline curve as will be clearly shown below, it can be easily removed

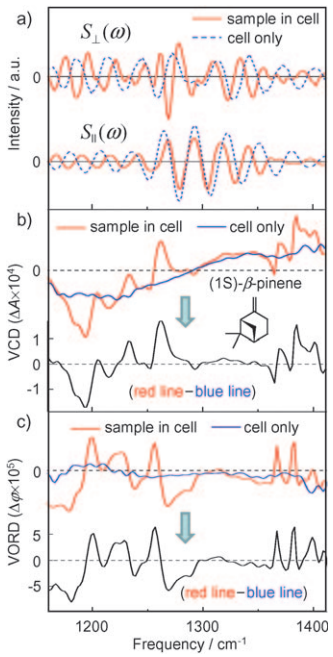

Figure 2. a) Heterodyned spectral interferograms, $S_\perp$ (upper) and $S_{||}$ (lower) of (1S)-β-pinene in the cell (red solid) and the cell only (blue dashed). The lower spectra are properly factorized for comparison with the upper spectra. b) Upper: Retrieved VCD spectra of (1S)-β-pinene in the cell (red) and the cell only (blue) from the spectral interferograms in (a). Lower: Baseline-corrected VCD spectrum obtained by subtracting the blue line from the red. c) Corresponding VORD spectra (upper) and baseline-corrected one (lower).

from the VCD or vibrational ORD (VORD) spectra of sample plus cell.

Once $S_\perp$ and $S_{||}$ are obtained, the VCD (ΔA) and VORD ($\Delta\varphi$) spectra can be simultaneously retrieved by the following conversion shown in Equations (1) and (2)[8–10]

$$\Delta A(\omega) = \frac{4}{2.303}\mathrm{Im}\left[\frac{F[\theta(t)F^{-1}\{S_\perp(\omega)\}]}{F[\theta(t)F^{-1}\{S_{||}(\omega)\}]}\right], \quad (1)$$

$$\Delta\varphi(\omega) = \mathrm{Re}\left[\frac{F[\theta(t)F^{-1}\{S_\perp(\omega)\}]}{F[\theta(t)F^{-1}\{S_{||}(\omega)\}]}\right]. \quad (2)$$

Here $F(\ldots)$ and $F^{-1}(\ldots)$ denote the Fourier and inverse Fourier transformations, respectively, and $\theta(t)$ is the Heavyside-step function. The converted VCD spectrum of (1S)-β-pinene (red) with Equation (1) is plotted together with that of the cell only (blue) in the upper panel of Figure 2b. The former shows highly structured VCD bands, whereas the latter exhibits a featureless smooth baseline. Note that the overall distortion of the red line in Figure 2b nearly follows the blue. By subtracting this instrumental effect (blue) from the combined (red), the VCD spectrum of the sample only (black) can be extracted. This is in a good agreement with the experimental result measured with a cw FT-IR VCD spectrometer.[16] Figure 2c depicts the corresponding VORD spectra retrieved by Equation (2) and clearly shows that the cell-polarizer contribution (blue) is negligible in the real part spectrum though it appears

comparable to the chiral signal of the sample itself in the spectral interferograms (see the upper in Figure 2a). From the present experimental results, it is believed that i) the present setup employing the home-made BAGP's is quite reliable and ii) the instrumental effect caused by optical imperfection of the polarizers and the cell can easily be eliminated.

In summary, the chevron geometry Brewster's angle germanium polarizer has ultimate extinction ratio that is suitable for wide applications of the cross-polarization VOA FID measurement technique covering the entire IR frequency range. Measuring the VCD spectrum of the C–C stretch vibrational modes of (1S)-β-pinene, we successfully demonstrated that the spectral limitation imposed by the dichroic calcite polarizer used in our previous attempts[9,10] has been overcome. It is believed that the present technique will be a promising tool for a variety of time-resolved VCD studies of chemical reactions involving chiral molecules and of protein structure and dynamics in the future.

Experimental Section

As a light source, femtosecond IR pulse with 8 μm center wavelength is generated by difference frequency mixing of signal and idler pulses from an optical parametric amplifier (OPA-800C, Spectra Physics) at a 0.5 mm-thick $AgGaS_2$ crystal with type II phase-matching. The beam divergence is controlled to be less than 35-mrad half-angle by properly positioning a collimating lens. Three Brewster's angle germanium polarizers are employed to perform the heterodyne-detections of both chiral and achiral FID signal fields from the chiral sample. For the chiral VOA FID ($E_\perp$) measurement, the transmission axis of the BAGP1 is vertically aligned and both BAGP2 and BAGP0 are horizontally aligned with respect to the optical table plane. To find an optimal cross-polarization configuration, the BAGP1 is mounted on a motorized rotational stage and then its rotation is finely controlled with 0.0005° angle resolution. A wire-grid polarizer in the reference arm of the interferometer serves as not only polarization rotator but also attenuator preventing the detector saturation. For the achiral FID ($E_{||}$) measurement, only the BAGP1 is slightly rotated by 0.5° with the others being fixed. In addition, to remove the homodyne signal of the reference field (E_{ref}) and to detect the heterodyne signal only, an optical chopper synchronized with the laser is introduced in the signal arm of the interferometer. Then, the signal detected at a single MCT (mercury cadmium telluride) detector via a monochromator is lock-in amplified and recorded as a spectral interferogram. From the perpendicular- and parallel-detected spectral interferograms ($S_{\perp,||}$), the VCD and VORD spectra are finally retrieved through a standard retrieval procedure [Equations (1) and (2)]. A more detailed experimental scheme and stepwise Fourier transformation procedure are found in the Supporting Information (see Figure S2 and S3) and ref. [10].

Acknowledgements

We thank the support from Creative Research Initiatives (CMDS) of MEST/KOSEF (M.C.) and KBSI grant (T29720) (S.-J. J.).

Keywords: chiral molecules · circular dichroism · free-induction-decay · optical activity

[1] L. D. Barron, *Molecular Light Scattering and Optical Activity, 2nd ed.*, Cambridge University Press, Cambridge, **2004**.
[2] N. Berova, K. Nakanishi, R. W. Woody, *Circular Dichroism: Principles and Applications, 2nd ed.*, Wiley-VCH, New York, **2000**.
[3] T. B. Freedman, X. L. Cao, R. K. Dukor, L. A. Nafie, *Chirality* **2003**, *15*, 743–758.
[4] P. J. Stephens, F. J. Devlin, J. J. Pan, *Chirality* **2008**, *20*, 643–663.
[5] P. Pancoska, S. C. Yasui, T. A. Keiderling, *Biochemistry* **1991**, *30*, 5089–5103.
[6] L. Wang, L. Yang, T. A. Keiderling, *Biophys. J.* **1994**, *67*, 2460-2467.
[7] J.-H. Choi, H. Lee, K. K. Lee, S. Hahn, M. Cho, *J. Chem. Phys.* **2007**, *126*, 045102.
[8] H. Rhee, J.-H. Ha, S.-J. Jeon, M. Cho, *J. Chem. Phys.* **2008**, *129*, 094507.
[9] H. Rhee, Y.-G. June, J.-S. Lee, K.-K. Lee, J.-H. Ha, Z. H. Kim, S.-J. Jeon, M. Cho, *Nature* **2009**, *458*, 310–313.
[10] H. Rhee, Y.-G. June, Z. H. Kim, S.-J. Jeon, M. Cho, *J. Opt. Soc. Am. B* **2009**, *26*, 1008–1017.
[11] T. J. Bridges, J. W. Klüver, *Appl. Opt.* **1965**, *4*, 1121–1125.
[12] J.-H. Choi, H. Lee, K.-K. Lee, S. Hahn, M. Cho, *J. Chem. Phys.* **2007**, *126*, 045102.
[13] R. A. G. D. Silva, J. Kubelka, P. Bour, S. M. Decatur, T. A. Keiderling, *Proc. Natl. Acad. Sci. USA* **2000**, *97*, 8318–8323.
[14] J.-H. Choi, S. Hahn, M. Cho, *Biopolymers* **2006**, *83*, 519–536.
[15] D. J. Dummer, S. G. Kaplan, L. M. Hanssen, A. S. Pine, Y. Zong, *Appl. Opt.* **1998**, *37*, 1194–1204.
[16] C. Guo, R. D. Shah, R. K. Dukor, T. B. Freedman, X. Cao, L. A. Nafie, *Vib. Spectrosc.* **2006**, *42*, 254–272.

Received: May 4, 2009
Published online on July 16, 2009

